Circulation: Arrhythmia and Electrophysiology

ORIGINAL ARTICLE

Novel CineECG Derived From Standard 12-Lead ECG Enables Right Ventricle Outflow Tract Localization of Electrical Substrate in Patients With Brugada Syndrome

Peter M. van Dam, PhD*; Emanuela T. Locati, MD, PhD*; Giuseppe Ciconte, MD; Valeria Borrelli, PhD; Francesca Heilbron, MD; Vincenzo Santinelli, MD; Gabriele Vicedomini, MD; Michelle M. Monasky, PhD; Emanuele Micaglio, MD; Luigi Giannelli, MD; Valerio Mecarocci, MD; Žarko Ćalović, MD; Luigi Anastasia, PhD; Carlo Pappone, MD, PhD

BACKGROUND: In Brugada syndrome (BrS), diagnosed in presence of a spontaneous or ajmaline-induced type-1 pattern, ventricular arrhythmias originate from the right ventricle outflow tract (RVOT). We developed a novel CineECG method, obtained by inverse electrocardiogram (ECG) from standard 12-lead ECG, to localize the electrical activity pathway in patients with BrS.

METHODS: The CineECG enabled the temporospatial localization of the ECG waveforms, deriving the mean temporospatial isochrone from standard 12-lead ECG. The study sample included (1) 15 patients with spontaneous type-1 Brugada pattern, and (2) 18 patients with ajmaline-induced BrS (at baseline and after ajmaline), in whom epicardial potential duration maps were available; (3) 17 type-3 BrS pattern patients not showing type-1 BrS pattern after ajmaline (ajmaline-negative); (4) 47 normal subjects; (5) 18 patients with right bundle branch block (RBBB). According to CineECG algorithm, each ECG was classified as Normal, Brugada, RBBB, or Undetermined.

RESULTS: In patients with spontaneous or ajmaline-induced BrS, CineECG localized the terminal mean temporospatial isochrone forces in the RVOT, congruent with the arrhythmogenic substrate location detected by epicardial potential duration maps. The RVOT location was never observed in normal, RBBB, or ajmaline-negative patients. In most patients with ajmaline-induced BrS (78%), the RVOT location was already evident at baseline. The CineECG classified all normal subjects and ajmaline-negative patients at baseline as Normal or Undetermined, all patients with RBBB as RBBB, whereas all patients with spontaneous and ajmaline-induced BrS as Brugada. Compared with standard 12-lead ECG, CineECG at baseline had a 100% positive predictive value and 81% negative predictive value in predicting ajmaline test results.

CONCLUSIONS: In patients with spontaneous and ajmaline-induced BrS, the CineECG localized the late QRS activity in the RVOT, a phenomenon never observed in normal, RBBB, or ajmaline-negative patients. The possibility to identify the RVOT as the location of the arrhythmogenic substrate by the noninvasive CineECG, based on the standard 12-lead ECG, opens new prospective for diagnosing patients with BrS.

GRAPHIC ABSTRACT: A graphic abstract is available for this article.

Key Words: ajmaline ■ Brugada syndrome ■ bundle branch block ■ electrocardiogram ■ sudden cardiac death ■ vectorcardiography

Correspondence to: Emanuela T. Locati, MD, PhD, Department of Arrhythmology and Electrophysiology, IRCCS Policlinico San Donato, Piazza E. Malan 2, 20097 San Donato Milanese, Milano, Italy. Email emanuelateresina.locati@grupposandonato.it

*Drs van Dam and Locati contributed equally to this work.

The Data Supplement is available at https://www.ahajournals.org/doi/suppl/10.1161/CIRCEP.120.008524.

For Sources of Funding and Disclosures, see page 1018.

Circulation: Arrhythmia and Electrophysiology is available at www.ahajournals.org/journal/circep

WHAT IS KNOWN?

- In Brugada syndrome, diagnosed in presence of a spontaneous or ajmaline-induced type-1 pattern, ventricular arrhythmias have been shown to originate from the right ventricle outflow tract.
- To date, the right ventricle outflow tract localization could only be demonstrated by complex mapping methods, either by body surface mapping requiring the acquisition of 250 electrodes or by invasive epicardial isopotential mapping.

WHAT THE STUDY ADDS?

- The cineECG, derived from 12-lead ECGs by an inverse ECG method, enabled the temporospatial localization of the ECG waveforms to a 3-dimensional heart model.
- In Brugada patients, the terminal components of the ventricular depolarization were localized to the right ventricle outflow tract, congruent with the localization of the arrhythmogenic substrate detected by epicardial potential duration maps.
- The right ventricle outflow tract localization of the QRS terminal components never occurred in normal subjects and in right bundle branch block patients, while it was present already at baseline in patients who developed type-1 Brugada pattern during ajmaline infusion.

Nonstandard Abbreviations and Acronyms

BrS	Brugada syndrome
LV	left ventricle
mTSI	mean temporal-spatial isochrones
PDM	potential duration maps
RBBB	right bundle branch block
RV	right ventricle
RVOT	right ventricular outflow tract
TCR	transcardiac ratio
VA	ventricular arrhythmias

Brugada syndrome (BrS) is an inherited disorder associated with a high risk of sudden unexpected death due to ventricular arrhythmias (VA) in young and otherwise healthy patients with apparently normal hearts.[1–3] The diagnosis of BrS is achieved in the presence of either a spontaneous or drug-induced type-1 Brugada pattern in the 12-lead electrocardiogram (ECG),[1–3] characterized by a typical coved elevation of the ST interval specifically observed in V1-V2 precordial leads.[4] The *SCN5A* gene is currently the most frequently involved, accounting for about 30% of BrS cases,[4] but several other genes have also been advocated.[5]

In patients with BrS, the cardiac electrophysiological substrate was specifically localized at the epicardial level of the outflow tract of the right ventricular outflow tract (RVOT).[6,7] So far, this localization could only be demonstrated by complex mapping methods, either by body surface mapping requiring the acquisition of 250 electrodes[6] or by invasive epicardial isopotential mapping.[7,8]

In patients with spontaneous or ajmaline-induced BrS, epicardial electro-anatomic voltage maps can detect the arrhythmic substrate, characterized by prolonged fragmented ventricular potentials, generally located on the upper part of the anterior wall of the right ventricle (RV), which represents the area where malignant VA are originated.[7,8] The substrate area is variable in different patients with BrS before and after provocative test with ajmaline, and the extent of the substrate area is correlated with the risk of VA.[8] The substrate area can be ablated by epicardial radiofrequency application, after which the inducibility of VA is dramatically reduced, the typical type-1 Brugada pattern is abolished, and VA can no longer be induced by ajmaline infusion.[8]

Our previous findings showed that in patients with BrS, the epicardial substrate area was highly correlated with the finding of signal-averaged late potentials, which could be viewed as an expression of abnormal epicardial electrical activity.[9] Furthermore, although for many years BrS was considered a purely electric disease, our recent findings showed that the typical BrS pattern reflects an extensive RV arrhythmic substrate, even associated with consistent RV mechanical abnormalities, and that substrate ablation abolished both the Brugada pattern and mechanical abnormalities.[10]

In many clinical conditions, the QRS duration taken from 12-lead ECG is a relevant discriminator between normal and pathological activation sequences. However, although the QRS onset is generally easily detected, the QRS offset is often blurry and therefore difficult to ascertain, particularly in patients with right bundle branch block (RBBB) or in patients with BrS. However, the study of these late QRS components is crucial for the detection and discrimination of such conditions. Furthermore, the 12-lead ECG interpretation is indeed a complex pattern recognition, which does not directly associate waveforms with specific cardiac structures.

Therefore, we developed a new method to measure and localize the direction of the electrical activity occurring during QRS including the early phase of the ST segment. This novel cine ECG method utilizes the inverse ECG approach,[11,12] and combines ECG data with the cardiac anatomy, with the aim to overcome and facilitate the interpretation of the waveforms of the standard 12-lead ECG.

The diagnosis of BrS is often based on the ajmaline (or Flecainide) provocative test in patients who show suspicious type-2 or type-3 BrS patterns on baseline ECG but because of the potential induction of ventricular arrhythmias, those tests should be performed under continuous medical surveillance with advanced life-support

facilities. Therefore, the development of a method that might improve the interpretation and the diagnostic value of the standard 12-lead ECG is quite needed.

The aim of this study is to utilize the novel CineECG to localize the electrical activity pathway to specific cardiac areas in patients with spontaneous or ajmaline-induced BrS, in comparison with normal controls, with patients with RBBB, and with patients with type-3 Brugada pattern who did not develop the type-1 Brugada pattern after ajmaline infusion (defined as ajmaline negative patients).

METHODS

Study Sample

The study sample included in this study was derived from the about 2500 patients referred for suspected Brugada Syndrome to the Arrhythmology and Electrophysiology Unit, San Donato Hospital, Milan, Italy, in the last 5 years. Complete medical history, physical examination, and baseline ECGs were available in all the referred patients. Patients with confirmed Brugada syndrome diagnosis were included in the San Donato BrS Registry, now including about 1500 patients. Definitions used to define Brugada patterns were derived from the latest Brugada Consensus Document.[4] Full details of the rationale and design of the BrS registry have been previously published.[1,7,8] The BrS Registry protocol was reviewed and approved by the local Institutional Review Board, and all participants provided written informed consent.[7,8]

Brugada Patients

The Brugada patient group included 15 patients with spontaneous type-1 Brugada pattern (mean age 40+9 years, 100% males) and 18 patients with suspicious type-2 or type-3 Brugada pattern at baseline who developed type-1 Brugada pattern during ajmaline provocative test (ajmaline-induced BrS patients, 40+9 years, 80% males). Their baseline and after ajmaline ECG tracings were included in this analysis. All the included 33 patients with BrS had previously undergone an electrophysiological testing, had resulted inducible for sustained ventricular arrhythmias, and received an implantable cardioverter-defibrillator implantation. Most of these patients had a previous history of syncope or cardiac arrest (49%), and most patients had a familial history of unexplained juvenile sudden death (63%). These proportions were not significantly different between spontaneous and ajmaline-induced patients with BrS. All the included patients with BrS were studied before the acquisition of invasive epicardial mapping before epicardial ablation for BrS substrate,[7,8] and their epicardial duration maps were used for the correlation with the CineECG.

Ajmaline-Negative Patients

The ajmaline-negative patient group included 17 patients who underwent a clinical workup at our Hospital for suspicious type-3 Brugada pattern at baseline but did not develop a type-1 pattern during ajmaline test (ajmaline-negative patients, mean age 36±15 years, 30% males). Both baseline and after ajmaline ECG tracings were included in the analysis. A familial history of BrS was present in 88% of those patients, a familial history of juvenile sudden death in 16%, none had a previous history of cardiac arrest, and 12% had previous history of unexplained syncope.

All ECG tracings recorded in patients with BrS were collected by a customized electrode placement system, optimized for the detection of the BrS pattern, as shown in Figure 1A.[7,8] The ECG tracings were acquired in digital format by the Workmate Claris system of Abbot-St. Jude. In patients with BrS (spontaneous and ajmaline-induced), the 12-ECG tracings utilized in this study were obtained in concomitance with the procedure of acquisition of the combined endo-epicardial mapping (see below).

Control ECG Tracings

As reference for normal or RBBB QRS activation, we utilized the digital ECG tracings derived from the certified Physionet PTB Diagnostic ECG Database https://www.physionet.org/content/ptbdb/1.0.0/,[13] and ECG tracings selected from our San Donato Hospital out-patient clinic, recorded in digital format by Mortara Scribe ECG system. All normal and RBBB tracings were obtained with the standard electrode placement system. All ECG tracings were manually reviewed by 2 expert cardiologists (Drs Locati and Ciconte). A total of 65 ECG tracings were included as controls for this study, from 47 normal subjects (mean age 43+15 years, 75% males) and 18 patients with complete RBBB (mean age 69+15 years, 72% males).

Inverse ECG Methodology

To quantify the cardiac activation pathway, we used the inverse ECG method, previously described.[11] The cardiac activation pathway of the ventricles represents the average position of all electrically active myocardial tissue during the QRST complex. To construct the cardiac pathway, also referred to as the mean temporal-spatial isochrone (mTSI), a model of the ventricles is required in combination with the electrodes positioned on the thorax. For this analysis, we utilized a standard thorax/heart model (Figure 1A), to correlate the cardiac activation pathway to the cardiac anatomy. From this torso/heart model, the inverse ECG method computes the vectorcardiogram from the recorded 12-lead ECG, taking into account the electrode positions on the thorax and providing the mean direction of cardiac activation over time (Figure 1A). The mTSI, derived from the vectorcardiogram, represents the mean trajectory of the cardiac activation pathway, with the mid left septum as starting point (Figure 2). The mTSI is used to determine the progression of the cardiac activity to specific areas of the cardiac anatomy, such as the right or left chambers, or the RVOT, and the moving trajectory of the mTSI was defined as CineECG.

QRST Definitions

For each 12-lead ECG tracing, the QRS duration and the mTSI derived parameters were computed from a single representative QRS complex. The QRS onset and offset and the T-wave offset were automatically determined from the root mean square of the ECG signals (Figure 1B). The QRS onset was determined as the point where the QRS amplitude started to increase steadily from baseline for at least 10 ms. The QRS offset was defined as the

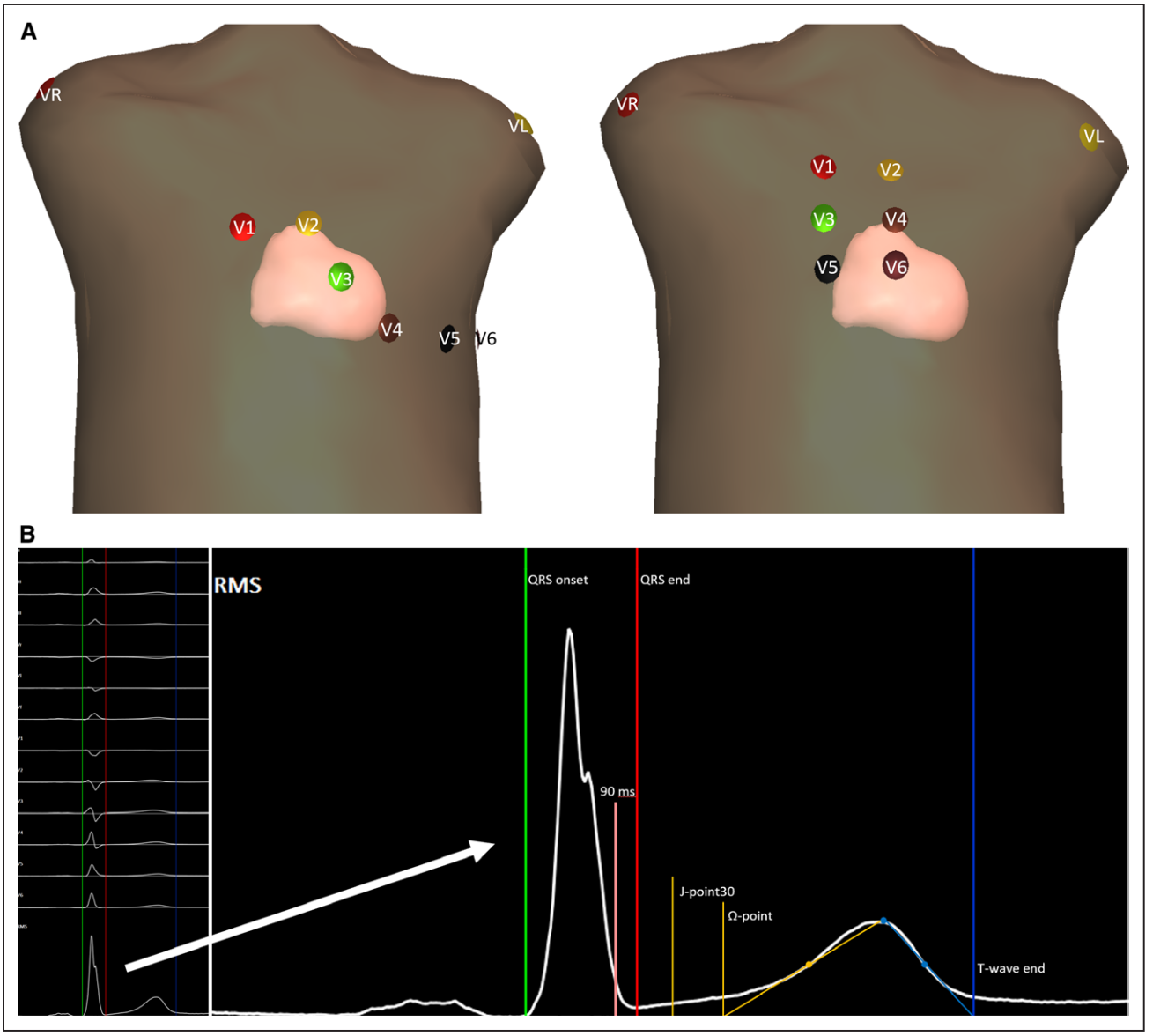

Figure 1. Model and fiducial points utilized to construct the 3-D cineECG.
A, The torso/heart model used with the 8 of the 9 electrode positions (the VF electrode is not shown). The torso/heart model on the left represents the standard 12-lead ECG configuration, used to analyze the PTB and clinical database ECGs. The torso/heart model on the right shows the model, with the adapted Brugada lead system. **B**, The fiducials of a single ECG beat from the 12-lead ECG were automatically derived from the root mean square (RMS) of all ECG signals measured. The QRS onset was defined as the time when subsequent ECG samples have an increasing value for at least 10 ms. The QRS offset was defined as the time when the RMS amplitude is lowest between 80 and 200 ms after the detected QRS onset. QRS90 was defined as the time 90 ms after QRS onset. J-Point 30 is defined as the time 30 ms after the QRS offset, and the Ω-point is defined by the intersection point at the time axis and the upslope tangent between the T peak and the midamplitude T wave (oranges lines). Similarly, the T-wave end is defined by the intersection point at the time axis and the downslope tangent between the T-wave peak and the mid–T-wave amplitude (blue lines). ECG indicates electrocardiogram; and PTB, *Physikalisch-Technische Bundesanstalt*, the National Metrology Institute of Germany, and is an open-access diagnostic digital ECG database.

first point with the lowest amplitude of the root mean square signal occurring between 80 and 200 ms after the onset. The T-wave offset was defined as the time axis intersection point of the line defined by the T-wave peak with the mid of the downslope T wave (Figure 1B). Noteworthy, in most cases of normal and RBBB tracings, the QRS offset can be reliably determined. For BrS tracings, the QRS offset is more difficult to be objectively defined. To overcome such difficulty, we introduced 3 additional time markers, relative to the terminal QRS electrical activity: (1) QRS90, that is, the QRS at 90 ms after the QRS onset, representing the cutoff for a normal QRS duration, (2) the J-point30, defined as the QRS offset (determined as the minimal root mean square voltage) plus 30 ms, and (3) the Ω-point, calculated from the intersection of the upslope of the T wave with the time axis (the same method used for the T-wave downslope, see Figure 1B).

Mean Temporospatial Isochrone

The mTSI, which represents the mean trajectory of the cardiac activation pathway, was defined to move through the heart with a constant velocity of 0.7 m/s in the 3-dimensional (3D) direction indicated by the vectorcardiogram $(\overrightarrow{VCG})$. The velocity of 0.7

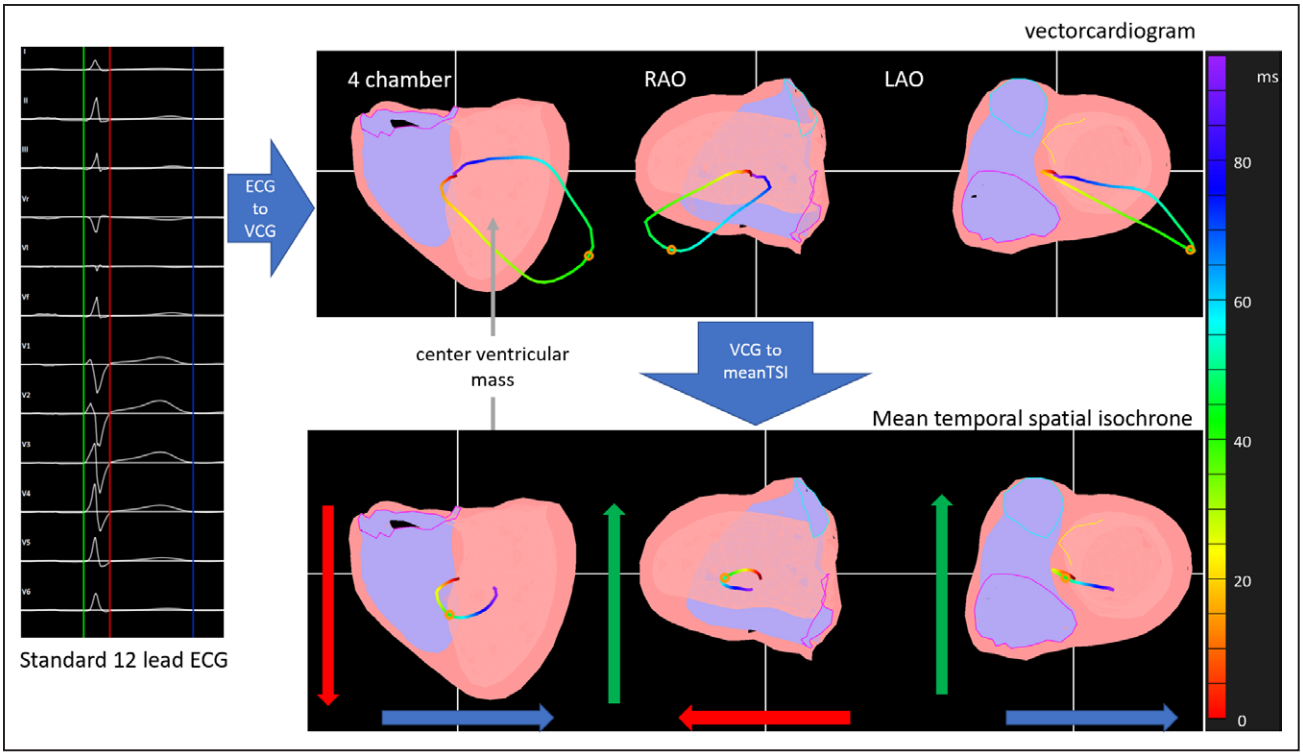

Figure 2. The CineECG work-flow in a normal subject.
The first step is to convert the 12-lead ECG into the vectorcardiogram (VCG), positioned at the center of ventricular mass, from which the mean temporal-spatial isochrone (mTSI) trajectory can be constructed (**lower** on the **right**). The ventricles are projected in three standard orientations: (1) 4 chambers, right anterior oblique (RAO), and left anterior oblique views (LAO). The right ventricle is indicated in transparent blue. The blue arrows indicate the right-to-left axis, the green arrow the posterior-to-anterior axis, and the red arrow the base-to-apex axis. The colors of the VCG and mTSI indicate the time from the QRS onset to the QRS offset (color bar on the **right**). The trans-septal vector is indicated in red. In this case, the transcardiac ratio is 11%, as the starting point (red) and the end point (purple) are very close. In this case, the mTSI is located for 55% of the QRS duration in the septal region, while for the 45% of the QRS duration in the left ventricle.

m/s is in the physiological range of the myocardial propagation velocity.[14,15] In detail: The $\overrightarrow{VCG}$, the direction of activation, is computed from the 9 electrodes, building the 12-lead ECG by the following equation:

$$\overrightarrow{VCG}(t) = \sum_{el=1}^{9} ecg_{el}(t) \cdot \alpha_{el} \left| r_{el} - mTSI(t-1) \right| \qquad (1)$$

where $\left| r_{el} - mTSI \right|$ is the normalized vector between the mTSI 3D-position in the heart and the electrode position on the thorax (r_{el}). The $ecg_{el}(t)$ is the value of the ECG at an electrode at time-sample t. Factor α_{el} was set to 0 for the x direction and 2 for the y and z directions for the unaugmented extremity leads (VR, VL, and VF). For all other leads, the α_{el} factor was set to 1 for all directions. This formula takes into account and corrects for the 2 different electrode placement systems utilized for patients with BrS and control ECG tracings. The movement of the mTSI is now defined by the direction of the vectorcardiogram and the previous mTSI position and a propagation velocity v. The mTSI position for $t>0$ (=QRS onset) is defined by the following equation:

$$mTSI(t) = mTSI(t-1) + v \frac{VCG(t)}{\|VCG(t)\|} \qquad (2)$$

In this study, all patients being in normal sinus rhythm, the cardiac activation starts in the left septum, close to the center of mass of the ventricles.[16,17] Thus, the center of mass of the ventricular model is used as the $mTSI(0)$ starting point. The mTSI is relatively insensitive to noise in the ECG/vectorcardiogram because it uses only the direction of the vectorcardiogram and not its amplitude. No additional signal processing on the mTSI is, therefore, required. Moreover, the computation of the CineECG is almost instantaneous (<200 ms) enabling its use also while recording the ECG.

CineECG Definitions

To visualize the tempo-spatial localization of the electrical activity pathway, we introduced the new concept of CineECG, representing the moving trajectory of the mTSI within the cardiac anatomic structures. To establish and visualize a quantifiable relation between the cardiac anatomy and the mTSI trajectory, 3 standard X-ray views on the heart were created from the heart model: a standard 4-chamber view and right and left anterior oblique views (right anterior oblique and left anterior oblique, Figure 2). Therefore, the terminal direction of the mTSI can be related to specific structures of the heart, like septum, and RV or left ventricle (LV) free walls, or RVOT. An example of the construction and visualization of the vectorcardiogram and mTSI for a normal activation is shown in Figure 2 and Movie I in the Data Supplement. In a normal subject, the $\overrightarrow{VCG}$ is mainly pointing towards the LV free wall, with a small initial trans-septal vector. In the mTSI trajectory, the trans-septal vector is clearly

visible. Moreover, the mTSI stays close to the septum ending in the midbase LV area.

CineECG Parameters

To quantify the cardiac activation pathway depicted by the CineECG, new quantitative parameters derived from mTSI were also defined:

- Transcardiac ratio (TCR): TCR is defined as the 3D-distance between the starting and the ending points of the mTSI, coincident with the QRS onset to the QRS offset. As this measure is potentially influenced by the size of the heart, it is weighted by the size of the heart model, resulting as a relative number. From our previous experience, normal cardiac activation is usually associated with a TCR generally well below 40%.[11] As an example, the TCR for the normal subject shown in Figure 2 was 11%.
- mTSI spatial location: At each time sample of the mTSI, its 3D-spatial localization in the heart is determined, and 3 cardiac areas were defined, either septal, LV, or RV. The initial spatial location of the mTSI is left septal, and it moves according to the direction determined by the vectorcardiogram. In case of normal activation, the mTSI initially moves trans-septal and then towards the LV, staying close to the septum (Figure 2). The spatial location is computed as the percentage of QRS duration spent by the mTSI in each of the 3 cardiac areas. As an example, in a normal subject, the mTSI is located for 55% of the QRS duration in the septum, for 45% in the LV, but never in the RV (Figure 2).
- Terminal mTSI direction: To measure the direction of the electrical activity occurring during the terminal phase of the QRS, or concealed within the ST segment, we computed the location of the terminal mTSI direction at the 3 time markers related to the end of QRS electrical activity as described above, ie, QRS90, J-point30, and Ω-point (Figure 1B). The terminal mTSI direction is quantified as a relative number between −1 and +1, indicating the congruence with the direction of any of the 3 cardiac axes (Figure 2).
- mTSI classification algorithm: Based on the QRS duration and on the above described mTSI parameters, a classification algorithm was developed to test the ability to discriminate tracings with spontaneous or ajmaline-induced type-1 BrS pattern from normal or RBBB tracings. Four diagnostic classes were defined: (1) Normal, (2) RBBB, (3) Brugada, and (4) Undetermined. For each class, a set of parameter values were used to compute the probability of a certain classification. The probability for a certain parameter is set to either 0 or 1, with 1 indicating the classification met, and 0 the classification not met. The classification was determined by the highest probability score. The following criteria were used to:
- Normal: QRS duration <110 ms, TCR 5% to 38%, terminal mTSI direction towards the LV basal area.
- RBBB: QRS duration 120–190 ms, TCR >50%, terminal mTSI towards RV basal area.
- Brugada: QRS duration >110 ms, TCR >50%, terminal mTSI, specifically defined for BrS between 110 and 180 ms after onset QRS, towards the RV free wall or RVOT (NOT towards the RV or LV basal area).
- Undetermined: Did not match any of the criteria above.

Electrophysiological Epicardial Mapping

All Brugada patients underwent a combined endo-epicardial mapping procedure using a 3D mapping system (CARTO 3, Biosense Webster, CA), as previously described.[7,8] All maps were obtained at baseline conditions and after drug challenge (ajmaline up to 1 mg/kg in 5 minutes). Total signal duration was measured for each potential before and after drug challenge as previously described.[7,8] Measurements were interpreted and validated online by 2 expert electrophysiologists using the CARTO3 system electronic caliper. The potential duration map (PDM) was created by collecting the duration of each electrogram. As a result, a color-coded map was obtained showing the regions displaying the shortest (red color) and the longest (purple color) durations. The electrical substrate area was defined as an area where abnormal electrograms were identified if they met at least one of the following characteristics: (1) a wide duration (>110 ms) with fragmented component (>3 distinct peaks); (2) late component of low-voltage amplitude ranging from 0.05 to 1.5mV; (3) distinct and delayed component exceeding the end of the QRS complex.[7,8]

Statistical Methods

Statistical analysis was conducted using the software IBM SPSS 1.0.0.1327. CineECG parameters, including QRS duration, TCR, mTSI Spatial Location (septal, LV, or RV), and terminal mTSI directions (at each of the 3 time markers, end of QRS electrical activity QRS90, J-point30, and Ω-point) were compared among the seven sample groups: Normal, RBBB, Spontaneous Brugada Pattern Type-1 Patients, Ajmaline-Induced Brugada Patients (at baseline and after ajmaline), and Ajmaline-Negative Patients (at baseline and after ajmaline).

Data were assessed using Shapiro Wilk ($P<0.05$), normality plots, and box plots. The null hypothesis of normal distribution was rejected for all the parameters ($P<0.001$). Data were provided as means, with 95% upper and lower CIs. The Kruskal-Wallis 1-way ANOVA for nonparametric data was, therefore, used to perform pairwise comparison between the different ECG diagnostic groups. The Bonferroni P value adjustment was applied to correct for multiple comparisons. Probability values <5% were considered significant.

RESULTS

In Table 1, we provide the quantitative results for all study groups for the CineECG parameters, specifically the mean QRS duration, the mTSI spatial location, the TCR, and the location of the terminal mTSI direction (from QRS90 to QRS offset). The full results of the statistical analysis are provided in the Data Supplement.

Normal Subjects

For the 47 normal subjects, the QRS duration was on average 90 ms (Table 1). The mTSI direction was generally pointing towards the LV basal area, and the mTSI trajectory was compact, resulting in a TCR with a median value

Table 1. CineECG Characteristics per Patient Group (Mean, 95% CI)

Patient Groups	No. of Patients	Test type	QRS Duration, ms	TCR %	mTSI Spatial Location %			Terminal mTSI Direction	
					Septum	LV	RV	To RVOT	To Base
Normal subjects	47	Baseline	90 (88/92)*†‡	23 (3–53)*	79 (45–100)†	21 (0–55)*	0 (0–3)*†	0.07 (–0.06/0.21)†§	–0.52 (–0.71/–0.33)*†‡
Patients with RBBB	18	Baseline	144 (135/152)*§‖	36 (31–59)*§‖	68 (43–100)	0 (0–44)*	22 (0–42)*§‖	0.03 (–0.05/0.12)	0.58 (0.39/0.78)*§
Patients with spontaneous type-1 Brugada pattern	15	Baseline	154 (137/171)†	26 (14–55)	68 (21–100)†	7 (0–63)	0 (0–79)†§	0.58 (0.38/0.79)†§	0.10 (–0.04/0.24)
Patients with ajmaline-induced Brugada pattern	18	Ajmaline	156 (146/166)†	29 (12–47)	74 (23–100)	0 (0–77)	3 (0–54)†§	0.64 (0.36/0.92)†§	0.24 (0.08/0.40)†
		Baseline	122 (115/130)†	24 (16–39)§	72 (39–100)	21 (0–62)	0 (0–50)§	0.4 (0.06/0.74)	–0.16 (–0.38/0.07)§
Ajmaline–negative patients	17	Ajmaline	121 (110/131)‡	26 (10–44)‖¶	72 (19–100)	24 (0–64)	0 (0–81)‖	0.4 (–0.01/81)	0.25 (–0.4/0.53)‡
		Baseline	100 (93/107)‖	16 (4–51)‖¶	83 (20–100)	15 (0–80)	0 (0–64)‖	0.42 (0.12/0.72)	0.12 (–0.14/0.39)‡

The descriptive statistics for every patient group of the QRS duration (mean and 95% CI in ms), the TCR (median and the range (minimum-maximum) in %), mTSI spatial location (median and the range [minimum-maximum] in %), and terminal mTSI direction quantified, all given as a relative number between -1 and +1 (mean and 95 % CI; see text for definitions). The Kruskal-Wallis 1-way ANOVA for nonparametric data was used to perform pairwise comparison between the different ECG diagnostic groups. The Bonferroni *P* value adjustment was applied to correct for multiple comparisons. LV indicates left ventricle; mTSI, mean temporospatial isochrone; RBBB, right bundle branch block; RV, right ventricle; RVOT, RV outflow tract; and TCR, transcardiac ratio.

Significant differences ($P<0.05$) for each comparison was indicated as follows:

*Comparison between normal subjects vs patients with RBBB

†Normal subjects vs either spontaneous or ajmaline-induced (baseline and after ajmaline) Brugada patients

‡Normal subjects vs noninducible patients (baseline and after ajmaline)

§RBBB patients vs with spontaneous type-1 or ajmaline-induced Brugada pattern (baseline and ajmaline)

‖RBBB vs ajmaline-negative patients (baseline and after ajmaline)

¶Baseline vs after ajmaline in both for ajmaline-induced and ajmaline-negative patients. Noteworthy, no significant differences were observed between with spontaneous type-1 or ajmaline-induced Brugada pattern (see Data Supplement for further details on the Statistical Analysis).

of 23% (Figure 3A). The CineECG illustrated the trajectory of the mTSI across the heart, showing an initial trans-septal vector, then moving to the left chamber (Movie I in the Data Supplement). Only 3 out of the 47 normal subjects (6%) had a TCR of >40%, which is considered large for an activation initiated by the His-Purkinje system (Figure 2). They partially overlapped the features of the RBBB and Brugada ECG patterns, although their QRS were <110 ms, and their terminal mTSI location was still in the left chamber. Among normal subjects, the CineECG classification came to a correct adjudication as Normal in 44 out 47 cases (94%): In 3 cases, all with larger than average TCR ratio the classification was Undetermined (Table 2).

Patients with RBBB

For the 18 patients with RBBB, the QRS duration was on average 144 ms (Table 1), significantly longer than normal subjects and ajmaline-negative patients, but not significantly different from spontaneous and patients with ajmaline-induced BrS. The median TCR value was 36%, and the CineECG generally showed an open-loop configuration (Figure 3B). As to the terminal mTSI in the 4 chamber and right anterior oblique projections, there was no overlapping between normal subjects and patients with RBBB.

Their CineECG showed an initial trans-septal vector, then moving towards the RV basal area, representing an activation going from the right apical region towards the right base of the heart (Movie II in the Data Supplement). According to the CineECG classification, all patients with RBBB on standard 12-lead ECG were correctly adjudicated as RBBB.

Spontaneous Type-1 Brugada Patients.

In the 15 patients with spontaneous type-1 Brugada pattern, the QRS duration was on average 154 ms, and the median TCR was 26%, with an open-loop configuration (Table 1). This was significantly higher than normal subjects, but not different from RRBB patients. Noteworthy, at a difference with normal and RBBB tracings, in spontaneous patients with BrS, the terminal mTSI direction was homogeneously directed towards the RVOT (Table 1, Figure 3C and Movie III in the Data Supplement).

The RVOT localization of the mTSI terminal activation detected by CineECG was congruent with the area of arrhythmogenic substrate detected by the potential duration maps (see Figure 4A). All spontaneous patients with BrS were correctly adjudicated to the Brugada classification (Table 2).

Ajmaline-Induced Brugada Patients

In the 18 patients with ajmaline-induced BrS, the QRS duration was 122 ms at baseline and significantly increased to 156 ms (Table 1). The mTSI always had an open-loop configuration, and the terminal mTSI direction was homogeneously directed towards the RVOT. Type-2

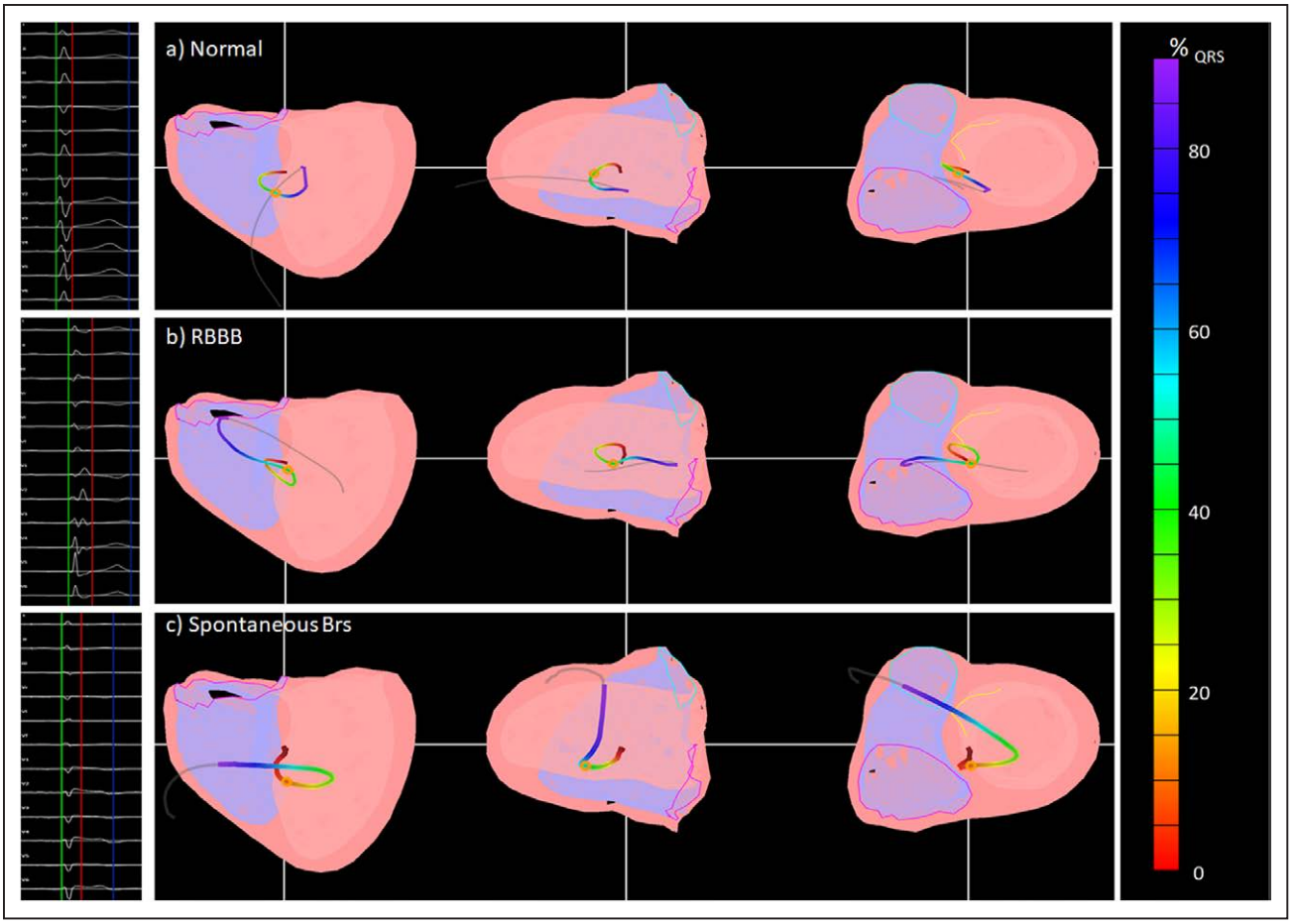

Figure 3. Three typical examples of the mean temporo-spatial isochrone (mTSI) trajectory.
mTSI is shown for a normal control (**A**); a patient with right bundle branch block (RBBB; **B**); and a patient with spontaneous type-1 Brugada pattern (**C**). In the patient with spontaneous type-1 Brugada pattern, the CineECG showed the terminal mTSI location in the right ventricle outflow tract. For each patient, the mTSI is shown by the colored line during the QRS, whereas the terminal mTSI (including T wave) is shown as a solid gray line, indicating also the terminal direction of the mTSI during the ST segment. The colors indicate the time during the QRS, red early, and purple late. BrS indicates Brugada syndrome.

BrS pattern was present in 5 patients, whereas type-3 BrS pattern in the remaining 13 patients.

In patients with ajmaline-induced BrS, the only significant difference between baseline and after ajmaline parameters was in the QRS duration, whereas all CineECG parameters were in the same range, and specifically, the terminal mTSI direction was mainly and homogeneously already directed towards the RVOT even at baseline (Table 1, Figure 5A and 5A and Movies IV and V in the Data Supplement). The mean spatial direction of the terminal mTSI, in the 4 chamber and right anterior oblique projections, had a similar behavior both in spontaneous and patients with ajmaline-induced BrS.

No significant differences between spontaneous or ajmaline-induced Brugada patients in most CineECG parameters were observed. In both groups, the RVOT localization of the mTSI terminal activation by CineECG was congruent with the area of arrhythmogenic substrate detected by the epicardial potential duration maps after ajmaline infusion (see Figure 4B and Movie V in the Data Supplement).

Noteworthy, by the CineECG method, 78% of the baseline ECG tracings of patients with ajmaline-induced BrS was already correctly classified as Brugada, and the remaining were classified either as Normal or Undetermined. After ajmaline, 100% were classified as Brugada.

Ajmaline-Negative Patients

In the 17 patients, all with type-3 Brugada pattern at baseline, who did not develop a typical type-1 Brugada pattern on the standard 12-lead ECG after ajmaline infusion (ajmaline-negative patients), the QRS duration was 100 ms at baseline and significantly increased to 121 ms after ajmaline (Table 1, Figure 5C and 5D). According to the CineECG parameters, none of these patients showed an RVOT localization of the mTSI terminal activation at baseline, so none was classified as Brugada, and all were classified as Normal or Undetermined. After ajmaline infusion, heterogeneous patterns were revealed by the CineECG because 41% were classified as Normal,

Table 2. MeanTSI Classification Accuracy per Patient Group

Patient group	Test type	Normal	RBBB	Brugada	Undetermined
Normal subjects (47)	Baseline	0.94 (44)	0	0	0.06 (3)
Patients with RBBB (18)	Baseline	0	1.00	0	0
Patients with spontaneous type-1 Brugada pattern (15)	Baseline	0	0	1.00	0
Patients with ajmaline-induced Brugada pattern (18)	Baseline	0.11(2)	0	0.78 (14)	0.11(2)
	Ajmaline	0	0	1.00 (18)	0
Ajmaline-negative patients (17)	Baseline	0.88 (15)	0	0	0.12 (2)
	Ajmaline	0.41 (7)	0.06 (1)	0.18 (3)	0.35 (6)

Classification is given as probability between 0 (no likelihood of diagnosis) and 1.0 (high likelihood of diagnosis). For Normal subjects, patients with RBBB, patients with spontaneous type-1 and ajmaline-induced Brugada pattern, the likelihood of diagnosis in the correct class was above 0.9 (90%). In 3 of the 47 normal subjects, the diagnosis was undermined, while all patients with RBBB, all the patients with spontaneous Brugada pattern and all patients with ajmaline-induced Brugada pattern were correctly classified as Brugada. Noteworthy, 78% of the baseline tracings of patients with ajmaline-induced Brugada pattern, only showing type-2 or 3 Brugada pattern, were already correctly classified as Brugada by CineECG parameters. In contrast, the Brugada pattern was never observed at baseline in those who were diagnosed as ajmaline-negative based on the standard 12-lead ECG after ajmaline infusion. mTSI indicates mean temporospatial isochrone; and RBBB, right bundle branch block.

6% were classified as RBBB, 35% were Undetermined, and 18% were classified as Brugada (Table 2).

DISCUSSION

Our novel CineECG method, developed from the mTSI derived from standard 12-lead ECG tracings, by combining ECG data with the cardiac anatomy, created a direct relation between the electrical signals and their anatomic cardiac sources. Our main finding was that the CineECG method showed that the temporospatial localization of the abnormal BrS activation is pointing towards the RVOT. This unique feature was observed both in spontaneous and in ajmaline-induced type-1 patients with BrS (both at baseline and during ajmaline), but it was never observed in normal subjects,

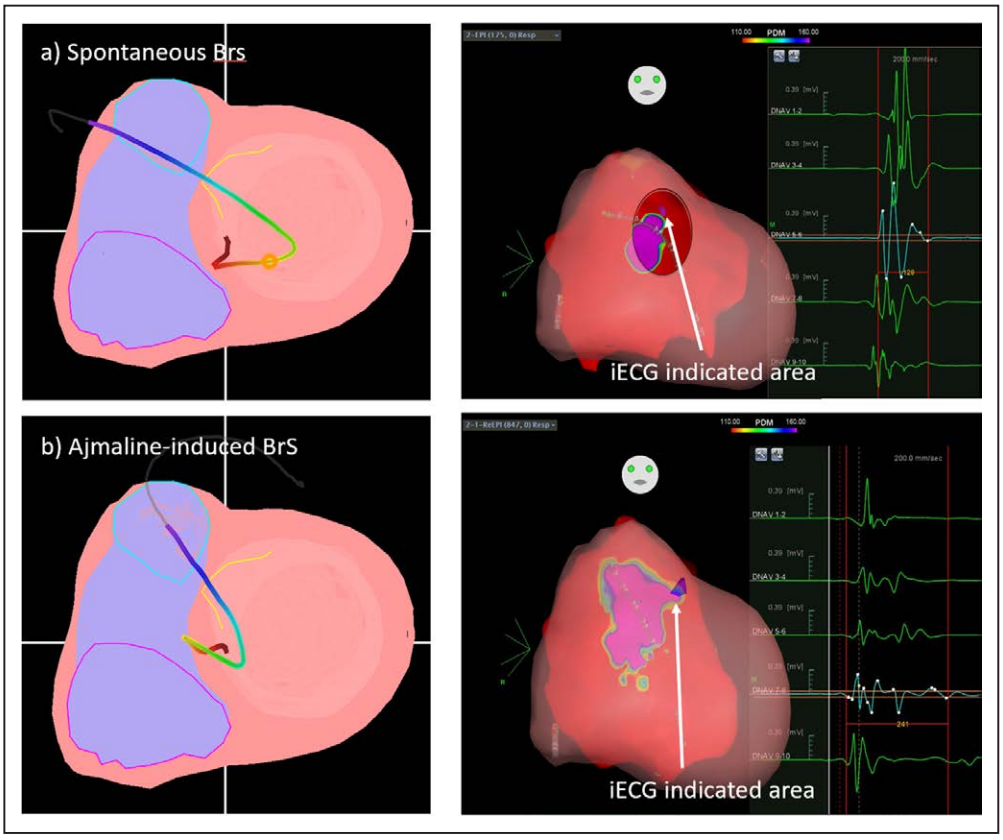

Figure 4. Epicardial potential duration maps (PDMs) of two patients with Brugada Syndrome (BrS).
The first is a patients with spontaneous type-1 Brugada pattern (**A**) and the second a patient with ajmaline-induced Brugada pattern (**B**). PDMs and 12-lead ECG tracings were obtained simultaneously. The arrhythmogenic substrate area is indicated in purple. In both cases, the locations of the substrate area detected by the PDM and the location of the terminal mean temporospatial isochrone by CineECG were coincident, in both cases located in the right ventricle outflow tract area. iECG indicates inverse ECG.

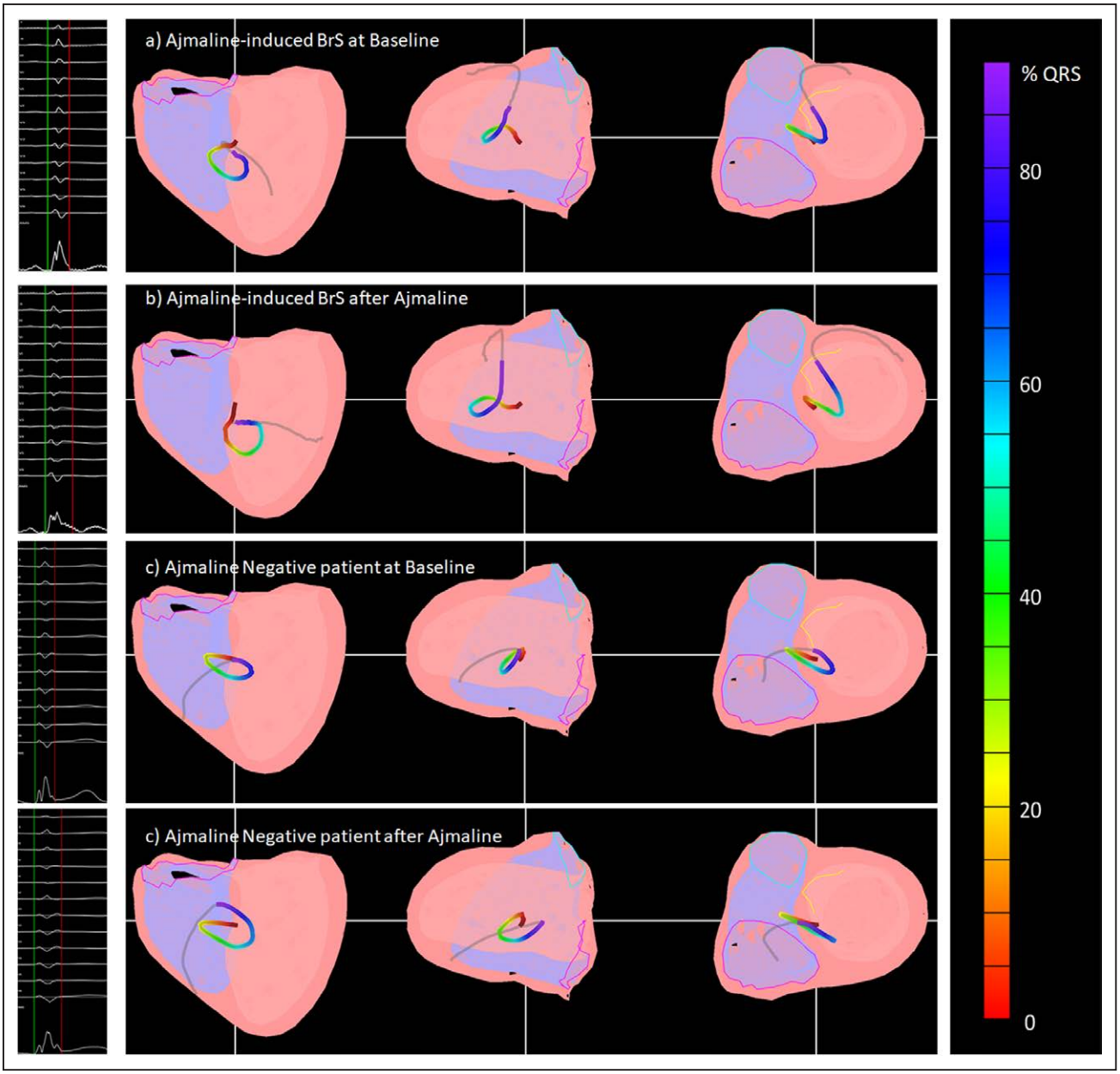

Figure 5. Typical examples of the mean temporospatial isochrone (mTSI) trajectory in 2 different patients with BrS. The mTSI is plotted for a patient with ajmaline-induced BrS at baseline (**A**) and after ajmaline (**B**) and for a ajmaline-negative patient at baseline (**C**) and after ajmaline (**D**). In the patient with ajmaline-induced BrS, the CineECG showed the terminal mTSI location in the right ventricle outflow tract, even if the 12-lead ECG tracing only showed type-2 BrS pattern. For the ajmaline-negative patient, the CineECG classified normal at baseline, and right bundle branch block after ajmaline. The mTSI is shown by the colored line during the QRS, whereas the terminal mTSI (including T wave) is shown as a solid grey line, indicating also the terminal direction of the mTSI during the ST segment. The colors indicate the time during the QRS, red early, and purple late.

nor in patients with RBBB, nor in ajmaline-negative patients at baseline.

The possibility to identify the RVOT location by our novel noninvasive CineECG, based on the elaboration of the readily available standard 12-lead ECG, opens an entirely new horizon for improving the diagnosis of patients with BrS. To date, the specific localization of the terminal QRS forces in the RVOT in patients with BrS could only be demonstrated by complex mapping methods, either by body surface mapping, requiring the acquisition of 250 electrodes,[6] or by invasive epicardial isopotential mapping.[7,8]

Interpretation of the CineECG

The trajectory of the mTSI represents the position of the average electrical forces at any given moment during the QRS, in relation to their cardiac sources. In normal subjects, the 2 ventricles are activated almost simultaneously, resulting in mTSI mainly located in the septal and

left ventricular area (Figure 3A and Movie I in the Data Supplement). In patients with RBBB, the initial forces are located in the left septum and in the LV, whereas the terminal mTSI was directed towards the right ventricular base (Figure 3B and Movie II in the Data Supplement). In patients with both spontaneous and ajmaline-induced type-1 BrS pattern, at baseline and after ajmaline, the initial forces are located in the left septum and in the LV, whereas the terminal mTSI is univocally directed towards the RVOT (Figure 3C, 4A, and 4B and Movies III, IV, and V in the Data Supplement). This typical behavior was already present at baseline in 78% of ajmaline-induced patients, in whom type-2 (in 5 cases) or type-3 Brugada pattern was present on the standard 12-lead ECG tracing.

The CineECG method, computed from standard 12-lead ECG, was able to show the same RVOT localization in patients with BrS, which was demonstrated by body surface mapping requiring 250 electrodes,[6] or by invasive epicardial isopotential mapping.[7,8] The CineECG method, at a difference with scalar ECG and body surface mapping, can also show the dynamic behavior of the mTSI within the heart model, correlating the cardiac electrical activity with its sources. Therefore, this method can improve the interpretation of the ECG waveforms and may open new horizons for the diagnostic and prognostic value of the standard 12-lead ECG. Possible clinical applications, besides the BrS, maybe the localization of accessory pathways, the interpretation of intraventricular conduction disorders, the evaluation of the resynchronization therapies, and maybe the localization of acute myocardial infarction.

Electrophysiological Basis of CineECG

The CineECG method provides the temporospatial trajectory of the summed electrical gradients, which may be due either to the activation or to the recovery process. Thus, the CineECG method cannot discriminate whether any terminal mTSI pathway is due either to a local slowing of the activation velocity or to early start of the ventricular recovery process.

More specifically, our results indicate that all patients with BrS had predominant electrical forces pointing towards the right ventricular outflow tract in the period corresponding to the terminal portion of the QRS and the initial phase of the ST segment. However, this method cannot discriminate whether this phenomenon was due to endo-to-epicardial activation delay, or to epi-to-endocardial early recovery forces. Further investigation, with more precise spatial reconstructions, may improve the understanding of the patho-physiologic mechanisms related to the CineECG model.

Congruence of RVOT Localization by CineECG and Epicardial Potential Duration Maps

In patients with BrS, the 12-ECG tracings utilized for this study were obtained in concomitance with the procedure of acquisition of the combined endo-epicardial mapping. In patients with both spontaneous or ajmaline-induced type-1 Brugada pattern, the epicardial potential duration mapping identified the location of the electrical substrate area in RVOT or RV anterior wall, concordant with the location of the terminal mTSI forces in RVOT, as illustrated by the CineECG (Figure 4A and 4B). Therefore, the CineECG can be viewed as a new noninvasive mapping system that may identify the presence and the anatomic location of the arrhythmogenic substrate in patients with BrS. This finding opens new perspectives for the diagnostic and prognostic evaluation of patients with BrS. In this view, a very promising new finding is the detection of the typical RVOT already present at baseline in the majority of patients with ajmaline-induced BrS, where the standard 12-lead ECG only showed nondiagnostic type-2 or type-3 pattern.

Comparison Between CineECG and Standard 12-lead ECG

Noteworthy, the CineECG already classified as Brugada 78% of the ajmaline-induced patients, who only had nondiagnostic type-2 or type-3 pattern on baseline ECG. In contrast, none of the ajmaline-negative patients was classified as Brugada. Therefore, at a difference with the standard 12-lead ECG, the CineECG obtained at baseline had high positive predictive value (100%) and negative predictive value (81%) in predicting the result of the ajmaline test. These results suggest that the novel noninvasive CineECG method, derived by a digital standard 12-lead ECG, may guide and limit the need to perform the ajmaline test. Notwithstanding these promising results, further studies, with a much higher number of patients, are required to determine the precise diagnostic value of the novel CineECG in detecting BrS.

Limitations

In this study, we used the standard heart/torso model to obtain the direct projection of the mTSI to the cardiac anatomy (Figure 1). In this study, the 12-lead ECGs of patients with BrS and controls were obtained with 2 different electrode placement configurations, and the CineECG method automatically corrected for the electrode position (see Equation 1 and Figure 1).[11] As future development, to take into consideration differences in individual thorax size and heart orientation, and to better localize the precise ECG electrode placement on the torso, we plan the use of a 3D camera to implement the thorax conformation into the algorithm and. This may increase the accuracy of temporospatial localization of the CineECG waveforms.[18]

Although the consistency of the CineECG behavior in each patient group supports the proof-of-concept and robustness of our method, further studies will be needed

to confirm these results, preferably with a method utilizing a personalized heart/torso model with customized electrode positions.

Conclusions

The novel CineECG method, starting from the standard 12-lead ECG tracing, computes the mean temporospatial isochrone, combining ECG data with the cardiac anatomy. This new CineECG was able to localize the late QRS electrical activity to RVOT in patients with BrS, both in spontaneous type-1 BrS pattern and in ajmaline-induced type-1 BrS pattern (both at baseline and after ajmaline), congruent with the anatomic localization of the arrhythmogenic substrate by the epicardial isopotential maps. A late QRS electrical activity to RVOT was observed neither in normal subjects nor in patients with RBBB or ajmaline-negative patients at baseline. The CineECG, derived from standard 12-lead ECG, can improve the understanding of the temporospatial localization of the electrical waveforms, thus may increase the diagnostic and prognostic accuracy of the standard 12-lead ECG not only in BrS but also in other cardiac arrhythmogenic diseases.

ARTICLE INFORMATION

Received January 3, 2020; accepted June 23, 2020.

Affiliations

Department of Cardiology, University Medical Center Utrecht, the Netherlands (P.M.v.D.). Department of Arrhythmology and Electrophysiology, IRCCS Policlinico San Donato, San Donato Milanese, Milan, Italy (E.T.L., G.C., V.B., V.S., G.V., M.M.M., E.M., L.G., V.M., Z.C., L.A, C.P.). ECG Excellence BV, Nieuwerbrug aan den Rijn, the Netherlands (P.M.v.D.). Vita-Salute San Raffaele University (L.A., C.P.). Milano Bicocca University, Istituto Auxologico Italiano San Luca, Milan, Italy (F.H.).

Acknowledgments

In memory of Michael Laks, his enthusiasm still drives the improvement of the standard 12-lead ECG diagnosis.

Sources of Funding

None.

Disclosures

Dr van Dam is an owner of Peacs BV and ECG Excellence BV. The other authors report no conflicts.

REFERENCES

1. Pappone C, Santinelli V. Brugada syndrome: progress in diagnosis and management. *Arrhythm Electrophysiol Rev.* 2019;8:13–18. doi: 10.15420/aer.2018.73.2
2. Priori SG, Blomström-Lundqvist C, Mazzanti A, Blom N, Borggrefe M, Camm J, Elliott PM, Fitzsimons D, Hatala R, Hindricks G, et al. 2015 ESC Guidelines for the management of patients with ventricular arrhythmias and the prevention of sudden cardiac death. *Rev Esp Cardiol (Engl Ed).* 2016;69:176. doi: 10.1016/j.rec.2016.01.001
3. Antzelevitch C, Patocskai B. Brugada syndrome: clinical, genetic, molecular, cellular, and ionic aspects. *Curr Probl Cardiol.* 2016;41:7–57. doi: 10.1016/j.cpcardiol.2015.06.002
4. Kapplinger JD, Tester DJ, Alders M, Benito B, Berthet M, Brugada J, Brugada P, Fressart V, Guerchicoff A, Harris-Kerr C, et al. An international compendium of mutations in the SCN5A-encoded cardiac sodium channel in patients referred for Brugada syndrome genetic testing. *Heart Rhythm.* 2010;7:33–46. doi: 10.1016/j.hrthm.2009.09.069
5. Gottschalk BH, Anselm DD, Brugada J, Brugada P, Wilde AA, Chiale PA, Pérez-Riera AR, Elizari MV, De Luna AB, Krahn AD, et al. Expert cardiologists cannot distinguish between Brugada phenocopy and Brugada syndrome electrocardiogram patterns. *Europace.* 2016;18:1095–1100. doi: 10.1093/europace/euv278
6. Zhang J, Sacher F, Hoffmayer K, O'Hara T, Strom M, Cuculich P, Silva J, Cooper D, Faddis M, Hocini M, et al. Cardiac electrophysiological substrate underlying the ECG phenotype and electrogram abnormalities in Brugada syndrome patients. *Circulation.* 2015;131:1950–1959. doi: 10.1161/CIRCULATIONAHA.114.013698
7. Chevallier S, Forclaz A, Tenkorang J, Ahmad Y, Faouzi M, Graf D, Schlaepfer J, Pruvot E. New electrocardiographic criteria for discriminating between Brugada types 2 and 3 patterns and incomplete right bundle branch block. *J Am Coll Cardiol.* 2011;58:2290–2298. doi: 10.1016/j.jacc.2011.08.039
8. Serra G, Baranchuk A, Bayés-De-Luna A, Brugada J, Goldwasser D, Capulzini L, Arazo D, Boraita A, Heras ME, Garcia-Niebla J, et al. New electrocardiographic criteria to differentiate the type-2 Brugada pattern from electrocardiogram of healthy athletes with r'-wave in leads V1/V2. *Europace.* 2014;16:1639–1645. doi: 10.1093/europace/euu025
9. Pappone C, Ciconte G, Manguso F, Vicedomini G, Mecarocci V, Conti M, Giannelli L, Pozzi P, Borrelli V, Menicanti L, et al. Assessing the malignant ventricular arrhythmic substrate in patients with brugada syndrome. *J Am Coll Cardiol.* 2018;71:1631–1646. doi: 10.1016/j.jacc.2018.02.022
10. Pappone C, Mecarocci V, Manguso F, Ciconte G, Vicedomini G, Sturla F, Votta E, Mazza B, Pozzi P, Borrelli V, et al. New electromechanical substrate abnormalities in high-risk patients with Brugada syndrome. *Heart Rhythm.* 2020;17:637–645. doi: 10.1016/j.hrthm.2019.11.019
11. van Dam PM. A new anatomical view on the vector cardiogram: the mean temporal-spatial isochrones. *J Electrocardiol.* 2017;50:732–738. doi: 10.1016/j.jelectrocard.2017.08.010
12. Roudijk R, Loh KP, van Dam PM. Mean temporal spatial isochrones direction as marker for activation delay in patients with arrhythmogenic cardiomyopathy. *Comput Cardiol.* 2018;45:1–4.
13. Bousseljot R, Kreiseler D, Schnabel A. Nutzung der EKG-signaldatenbank CARDIODAT der PTB über das internet. *Biomedizinische Technik / Biomedical Engineering.* 1995;40:317–318.
14. Kléber AG, Janse MJ, Wilms-Schopmann FJ, Wilde AA, Coronel R. Changes in conduction velocity during acute ischemia in ventricular myocardium of the isolated porcine heart. *Circulation.* 1986;73:189–198. doi: 10.1161/01.cir.73.1.189
15. Roberts DE, Hersh LT, Scher AM. Influence of cardiac fiber orientation on wavefront voltage, conduction velocity, and tissue resistivity in the dog. *Circ Res.* 1979;44:701–712. doi: 10.1161/01.res.44.5.701
16. Durrer D, van Dam RT, Freud GE, Janse MJ, Meijler FL, Arzbaecher RC. Total excitation of the isolated human heart. *Circulation.* 1970;41:899–912. doi: 10.1161/01.cir.41.6.899
17. van Dam PM, Oostendorp TF, Linnenbank AC, van Oosterom A. Non-invasive imaging of cardiac activation and recovery. *Ann Biomed Eng.* 2009;37:1739–1756. doi: 10.1007/s10439-009-9747-5
18. van Dam PM, Gordon JP, Laks M. Sensitivity of CIPS-computed PVC location to measurement errors in ECG electrode position: the need for the 3D camera. *J Electrocardiol.* 2014;47:788–793. doi: 10.1016/j.jelectrocard.2014.08.005